Molecular Recognition

DOI: 10.1002/ange.201300707

Chirped-Pulse and Cavity-Based Fourier Transform Microwave Spectra of the Methyl Lactate···Ammonia Adduct**

*Javix Thomas, Oleksandr Sukhorukov, Wolfgang Jäger, and Yunjie Xu**

Molecular recognition plays a vital role in biochemistry and biology. The efficiency of a molecular recognition process depends on the selectivity between the lock and the key molecules. Among intermolecular forces, hydrogen (H)-bonding interactions involving O, H, and N atoms are of particular interest because of their prominent roles in driving protein folding, molecular recognition, and other biochemical processes.[1] Studies of molecular recognition between a lock and a key molecule using jet-cooled rotational spectroscopy provide information for detailed understanding of the forces involved in a molecular recognition process. A small number of rotational spectroscopic studies of chiral lock–key systems have been reported before where the molecular subunits typically have only one H-binding site.[2,3] As a result, the selectivity between lock and key molecules is generally not specific enough, resulting in a good number of conformers separated only by very small energy differences.

To better mimic the unique specificity observed in biological systems, we select methyl lactate (ML), a chiral molecule with multiple functional groups and H-bond binding sites, as our lock, and ammonia as our key. The ML conformer with an intramolecular O−H···O=C H-bond is strongly favored over all other conformations.[4] It is of great interest to see if ammonia acts exclusively as a proton acceptor or donor, or if it plays a dual role in the ML···NH_3 adduct as there is a competition between intra- and intermolecular H-bonds. Such balance between the intra- and intermolecular H-bonding interactions is commonly encountered in biological systems and has a great influence on the selectivity between lock and key molecules.

Only a few NH_3-containing complexes have been studied so far by high-resolution spectroscopy. Ammonia generally acts as a proton acceptor, for example, in complexes with cyclopropane, methanol, and ethanol.[5-7] In complexes of ammonia with, for example, hydroquinone[8] and 7-hydroxy quinoline,[9] it serves both as a proton donor and acceptor. Only one chiral molecule–NH_3 adduct, namely glycidol···NH_3, was studied before using high-resolution spectroscopy.[10] Such studies of chiral–achiral adducts are of considerable relevance in light of the significant current interest in transfer of chirality from a chiral molecule to an achiral subunit through H-bonding interactions in solution and in a cold rare gas matrix.[11–13]

In this work, we report a detailed rotational spectroscopic study of the ML···NH_3 adduct, in combination with high-level ab initio calculations. The ML···NH_3 adduct is also unique in terms of its spectroscopy. First, this system has three internal rotors: two methyl rotors and one ammonia rotor. This is the first time to probe a molecular recognition process between a lock with two "spinning" tops and a key which is also a spinning top itself. Second, the ammonia rotor contains a quadrupolar ^{14}N nucleus. It therefore offers the opportunity to probe the distortion of the electric field gradient at the ^{14}N nucleus upon H-bonding with ML. Finally, the coupling of the internal rotations with the overall rotation of the complex may give rise to the first-order contributions from the off-diagonal elements of the ^{14}N nuclear quadrupole coupling tensor for lines with E internal rotor symmetry, allowing their determination experimentally.[14,15]

The spectral search for the binary adduct was carried out using a broadband chirped-pulse Fourier transform microwave (FTMW) spectrometer.[16] Broadband spectra of three different samples, namely ML, NH_3, and ML + NH_3, all in neon, were measured in the 7.7–10.4 GHz region using 10^6 averaging cycles. Transitions that require the presence of both ML and NH_3 could be readily identified. Five most stable binary ML···NH_3 adducts identified from ab initio calculations are summarized in Table 1. A 0.8 GHz section of a chirped-pulse MW spectrum is shown in Figure 1, together

Table 1: Relative energies and calculated spectroscopic constants of the five most stable ML···NH_3 conformers.

Conformers	I	II	III	IV	V
ΔD_e[a] [kJ mol^{-1}]	0.0	2.1	16.8	17.5	21.9
ΔD_o[b] [kJ mol^{-1}]	0.0	1.4	9.5	10.3	13.7
A [MHz]	2646	2207	3500	2290	1687
B [MHz]	1208	1389	894	1151	1584
C [MHz]	971	917	834	964	980
μ_a [D]	0.87	0.99	1.32	1.07	3.86
μ_b [D]	0.98	2.28	0.89	1.32	1.20
μ_c [D]	2.39	1.67	0.44	0.17	1.87
	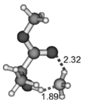	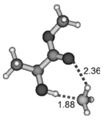	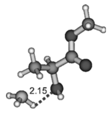	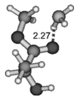	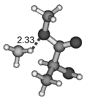

[a] Basis set superposition error (BSSE) corrected relative energies at the MP2/6-311 + + G(d,p) level. [b] Zero-point energy (ZPE) corrected.

---

[*] J. Thomas, Dr. O. Sukhorukov, Prof. Dr. W. Jäger, Prof. Dr. Y. Xu
Department of Chemistry, University of Alberta
Edmonton, AB, T6G2G2 (Canada)
E-mail: yunjie.xu@ualberta.ca

[**] This research was funded by the University of Alberta and the Natural Sciences and Engineering Research Council of Canada. Y.X. and W.J. are holders of Canada Research Chairs (Tier I). We thank Prof. H. Mäder for discussions concerning internal rotors and the XIAM program, and Prof. S. E. Novick and Dr. J. R. Cheeseman for nuclear quadrupole coupling constant calculations.

Supporting information for this article is available on the WWW under http://dx.doi.org/10.1002/anie.201300707.

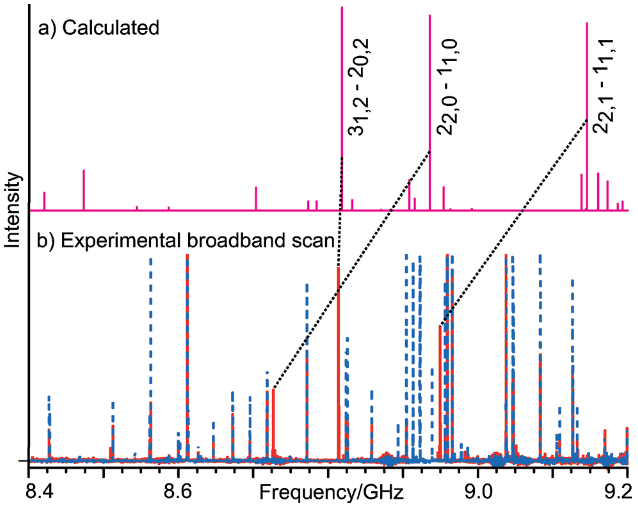

Figure 1. a) Simulated 0.8 GHz section of the rotational spectrum of ML···^{14}NH$_3$ **I** using the spectroscopic constants reported in Table 1 with $T_{rot} = 1$ K. b) 0.8 GHz sections of two broadband chirped-pulse microwave scans using ML + NH$_3$ + Ne (solid red) and ML + Ne (dashed blue) samples. The scan of NH$_3$ + Ne is not shown since the transitions observed are very weak in this frequency region.

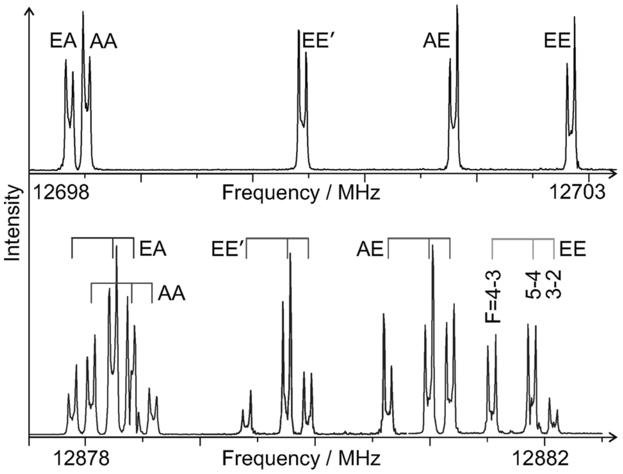

Figure 2. Experimental internal rotation and nuclear quadrupole hyperfine structures of the rotational transition $4_{2,2}$-$3_{1,2}$ of ML···^{15}NH$_3$ **I** (top) and ML···^{14}NH$_3$ **I** (bottom). Each spectrum is pieced together from four separate measurements.

with a portion of a simulated spectrum of conformer **I** using the ab initio spectroscopic constants and the Pgopher[17] program. The simulated intensity pattern does not match with the experimental data completely because of the omission of the ^{14}N nuclear quadrupole and the internal rotor splittings in the simulation.

To confirm the initial assignment and to unravel the complicated hyperfine structures, the final frequency measurements were done with a cavity-based FTMW instrument.[18] While splittings because of both the ester methyl internal rotation and ^{14}N nuclear quadrupole coupling were expected, an additional splitting was observed. This splitting is unlikely to be due to the second methyl rotor in ML since no such splitting was detected for the ML monomer.[4] One may hypothesize that the additional splitting arises from the NH$_3$ internal rotation motion even though one of the H atoms of NH$_3$ is H-bonded to ML. Indeed, an energy scan for the internal rotation of NH$_3$ provided an estimated barrier height of about 2.8 kJ mol^{-1} (see Figure S1 in the Supporting Information).

For simplification, ML···^{15}NH$_3$ was considered first. One expects five internal rotation components (j_1,j_2), namely AA = (0,0), EA = (1,0), AE = (0,1), EE = (1,1), and EE′ = (1,–1). Here j_1 and j_2 correspond to the internal rotation labels of the ester methyl group and NH$_3$, respectively, and the A/E notation indicates the symmetry species. The subsequent analysis of the ML···^{14}NH$_3$ **I** spectrum was aided by using a first-order nuclear quadrupole program. Complex hyperfine patterns of an example transition of the ^{15}NH$_3$ and ^{14}NH$_3$ isotopologues are shown in Figure 2.

The final global fits of both isotopologues were performed with the program XIAM,[19] currently the only program which can fit rotational transitions of a C_1 symmetry molecular system with multiple internal rotors and with additional nuclear quadrupole splitting. The Hamiltonian used can be written as Equation (1).

$$H = H_{rot} + H_{cd} + H_i + H_{ird} + H_{ii} + H_Q \tag{1}$$

Here, H_{rot} is the rigid rotor part, H_{cd} refers the centrifugal distortion part, H_i corresponds to the internal rotation part of the tops, H_{ird} accounts for the torsional state-dependent centrifugal terms, such as D_{pi2k}, H_{ii} is the top–top coupling term, such as F_{12}, and H_Q corresponds to the nuclear quadrupole coupling terms, such as χ_{aa} and χ_{bc}. The measured frequencies and the quantum number assignments of ML···^{15}NH$_3$ **I** and ML···^{14}NH$_3$ **I** are given in Tables S1 and S2 (see the Supporting Information), respectively. The spectroscopic constants obtained are summarized in Table 2, including the internal rotor parameters for both the ester methyl group and the NH$_3$ subunit and the diagonal nuclear quadrupole coupling constants of ^{14}N as well as one off-diagonal element.

The internal rotation barrier heights of the ester methyl group are 4.778(16) and 4.818(18) kJ mol^{-1} in ML···^{15}NH$_3$ and ML···^{14}NH$_3$, respectively, comparable to that of the monomer (4.76 kJ mol^{-1}).[4] This indicates that the replacement of the intramolecular H-bond by the intermolecular OH···NH···O=C H-bonds has little effect on the internal rotation of the ester methyl group. The experimental barrier heights for the ammonia internal rotation in ML···^{14}NH$_3$ and ML···^{15}NH$_3$ are 2.452(2) and 2.4538(7) kJ mol^{-1}, respectively. Since the NH$_3$ internal rotation is mainly hindered by the intermolecular OH···NH···O=C H-bonds, the magnitude of the barrier height is roughly proportional to the strength of the H-bond. For example, the NH$_3$ internal rotation barrier is 2.438 kJ mol^{-1} for the most stable glycidol···NH$_3$ conformer.[10] This suggests that the strength of the NH···O=C H-bond in ML···NH$_3$ is very similar to that in the most stable conformer of glycidol···NH$_3$. This similarity is also reflected in the corresponding moment-of-inertia values of the NH$_3$ top, which are related to the extent of the opening of the NH$_3$

Table 2: Experimental spectroscopic constants obtained for the ML···NH$_3$ adduct.

Parameter[a]	ML···^{14}NH$_3$		ML···^{15}NH$_3$	
A [MHz]	2576.6761(11)		2550.50192(65)	
B [MHz]	1219.23607(75)		1196.32952(25)	
C [MHz]	963.39221(55)		945.88376(22)	
D_J [kHz]	0.317(15)		0.2690(27)	
D_{JK} [kHz]	0.308(20)		0.409(31)	
D_K [kHz]	2.480(60)		2.421(53)	
d_1 [kHz]	−0.025(11)		−0.0567(19)	
d_2 [kHz]	−0.0220(39)		−0.0153(16)	
top	ester methyl group	ammonia	ester methyl group	ammonia
D_{pi2K} [MHz]	0.0	455.55(5)	0.0 (fixed)	457.0460(60)
D_{pi2-} [kHz]	0.0	−58.83(13)	0.0 (fixed)	−56.6210(31)
V [kJ^{-1} mol^{-1}]	4.778(16)	2.452(2)	4.818(18)	2.4538(7)
ρ	0.01285(4)	−0.006850(6)	0.012526(48)	−0.006793(1)
β [rad]	0.447(1)	1.87784(6)	0.4520(11)	1.91522(2)
γ [rad]	2.952(5)	2.9055(1)	2.95494(84)	2.90838(2)
F_0 [GHz][b]	155.33	181.76	156.42	181.67
F [GHz][b]	157.23	182.99	158.28	182.89
F_{12} [MHz][b]	−597.6		−562.01	
χ_{aa} [MHz][c]	1.480(1)		–	
χ_- [MHz][c]	−4.214(1)		–	
χ_{bc} [MHz][c]	1.3229(3)		–	
N	216		200	
σ [kHz]	3.6		4.9	

[a] Watson's S reduction[23] in the I^r representation. Physical significance of parameters, that is, which part of the Hamiltonian [Eq. (1)] they belong to, is provided in the Supporting Information. N is the number of transitions included in the fit, and σ is the standard deviation of the fit. [b] Derived from the fitted parameters. [c] The ab initio values for χ_{aa}, χ_-, and χ_{bc} are 1.6182, −4.6249, and 1.7260 MHz, and for the other two off-diagonal elements, χ_{ab} and χ_{ac}, are −0.7536 and 0.2699 MHz, respectively.

"umbrella". For ML···NH$_3$ **I**, these are 2.7805 (^{14}N) and 2.7817 uÅ^2 (^{15}N), compared to 2.7849 and 2.7885 uÅ^2 in the most stable glycidol···NH$_3$, respectively.

With the available experimental rotational constants, a partially refined r_0 structure was obtained where four H-bonding structural parameters were adjusted to reproduce the experimental rotational constants to about 50 kHz. The resulting values are listed in Table 3, together with the corresponding equilibrium values from the ab initio calculations.

Table 3: Partial refined r_0 geometry of the ML···NH$_3$ adduct.

ML···NH$_3$ I	r_e[a]	r_0[b]
fitted parameters		
N–O$_{OH}$ [Å]	2.858	2.887(5)
NO$_{OH}$–C [°]	109.26	110.58(1)
NO$_{OH}$–CC [°]	56.34	52.83(3)
HN–H$_{OH}$ [°]	93.90	97.(4)
derived H-bond distances		
N–HO [Å]	1.887	1.928
NH–O=C [Å]	2.325	2.359

[a] At the MP2/6-311++G(d,p) level. [b] See the text for details. Values in parentheses are errors in units of the last digit.

How much is the electric field gradient at the ^{14}N nucleus perturbed upon H-bonding to ML? There is not enough information to obtain the principal quadrupole coupling tensor components of ^{14}N in ML···NH$_3$ using the experimental χ constants only. Instead, we used the partial experimentally determined r_0-structure and calculated the direction cosine matrix for the principal χ constants at the MP2/6-311++G(d,p) level. The principal quadrupole coupling constants of ^{14}N thus obtained are $\chi_{xx} = 1.844$, $\chi_{yy} = 1.654$, and $\chi_{zz} = -3.497$ MHz, where x, y, and z are the principal quadrupole coupling axes of ^{14}N in the complex. While z is roughly along the OH···N H-bond direction, y is roughly in the plane of the NH···O H-bond. There is a substantial reduction in the magnitude of these constants in the z and y directions, whereas the change is smaller in the x direction, compared to the experimental $\chi_{zz} = -4.0890(1)$ and $\chi_{xx} = \chi_{yy} = 2.0450(1)$ MHz values of ^{14}NH$_3$.[20] This is not too surprising since the x direction is least effected by the formation of the OH···N and NH···C=O H-bonds. In the H$_3$N···hydrogen halide series where NH$_3$ serves only as a proton acceptor, a reduction was observed and attributed to the zero-point energy (ZPE) averaging of the large amplitude motions and a small electric perturbation at ^{14}N.[21] A similar amount of reduction was reported for glycidol···NH$_3$.[10] (Please note that there is a typo for the sign of χ_{zz} for glycidol···NH$_3$ and NH$_3$ in Ref. [10].) In addition, a 14.5 % reduction in χ_{zz} upon complexation with ML was predicted theoretically, in good agreement with the experimental observation. Such electric perturbation may be attributed to a small charge transfer facilitated by the cooperative effect of the OH···N and NH···C=O H-bonds. Indeed, a positive charge transfer of +0.026 e to the NH$_3$ subunit was calculated using natural bond-order (NBO) analysis[22] where the positive sign indicates a loss of electrons on NH$_3$.

Substantial efforts were made to locate the higher energy conformers of ML···NH$_3$ by analyzing the broadband rotational spectra of ML···^{15}NH$_3$ recorded with 2×10^6 cycles, but without success. While conformers **III** to **V** are predicted to be much less stable and therefore unlikely to be observed in a jet expansion, **II** is about 1.2 kJ mol^{-1} less stable and would be expected to be observed with the signal-to-noise ratio achieved for **I**. On the other hand, **II** differs only slightly from **I** (see Figure S2 for details) and the interconversion barrier was estimated to be lower than 1.4 kcal mol^{-1}.[13b] In a neon jet expansion, **II** is likely to relax to **I**, making **II** non-observable.

In conclusion, complex splitting patterns of the rotational transitions due to the internal rotations of the ester methyl group and the ammonia subunit, as well as the quadrupolar ^{14}N nucleus of ML···^{14}NH$_3$ and ML···^{15}NH$_3$ **I**, were observed and analyzed. The geometry of the adduct was refined using the experimental rotational constants. A detailed analysis of the nuclear quadrupole coupling tensor shows that the electric field gradient at ^{14}N in the binary adduct deviates noticeably from the cylindrical symmetry in the free NH_3 monomer and can be attributed to a small amount of charge transfer facilitated by the cooperative H-bonds. We plan to systematically increase the complexity of the amine key and to investigate the possible changes in the preferred H-binding sites as the amine key gets larger.

Experimental Section

Sample mixtures consisting of 0.06 % ML and 0.12 % NH_3 in neon at stagnation pressures of 4 to 8 bar were used. ML (99 %, Sigma Aldrich), $^{14}NH_3$ (98 %, Scott Speciality Gases Inc.), $^{15}NH_3$ (98 %, Cambridge Isotope Laboratories Inc.), and neon (99.9990 %) were used without further purification. The survey scans were carried out using a newly constructed chirped-pulse FTMW spectrometer[16] based on designs reported previously.[24] Briefly, a radiofrequency (rf) chirp (0.2–1 GHz 4 μs) generated by an arbitrary waveform generator (Tektronix AWG 710B) is mixed with the output of a MW synthesizer to produce a 2 GHz MW chirp in the 8–18 GHz range. These chirps are amplified with a 20 W solid-state MW amplifier (MW Power Inc., L0818-43) and then propagated into free space using a wide band, high gain, MW horn antenna (rf/MW instrumentation, ATH7G18). The resolution of the broadband spectrometer is 50 kHz. High-resolution measurements were done with a cavity-based[25] pulsed-jet FTMW spectrometer.[18] The frequency uncertainty is about 2 kHz and the full line width at half height is about 10 kHz.

All geometry optimization and harmonic frequency calculations were done using G03, while the nuclear quadrupole coupling constants and NBO analysis were done with the G09 program package[26] at the MP2/6-311++G(d,p) level. The basis set superposition error corrections were calculated using the counterpoise procedure of Boys and Bernardi.[27]

Received: January 27, 2013

Keywords: hydrogen-bonds · internal rotations · molecular recognition · rotational spectroscopy

---

[1] “Hydrogen Bonds in Proteins: Role and Strength”: R. E. Hubbard, M. K. Haider in *Encyclopedia of Life Sciences (ELS)*, Wiley, Chichester, **2010**.
[2] N. Borho, Y. Xu, *Angew. Chem.* **2007**, *119*, 2326; *Angew. Chem. Int. Ed.* **2007**, *46*, 2276; N. Borho, Y. Xu, *J. Am. Chem. Soc.* **2008**, *130*, 5916; J. Thomas, F. X. Sunahori, N. Borho, Y. Xu, *Chem. Eur. J.* **2011**, *17*, 4582.
[3] A. Maris, B. M. Giuliano, D. Bonazzi, W. Caminati, *J. Am. Chem. Soc.* **2008**, *130*, 13860.
[4] P. Ottaviani, B. Velino, W. Caminati, *Chem. Phys. Lett.* **2006**, *428*, 236; N. Borho, Y. Xu, *Phys. Chem. Chem. Phys.* **2007**, *9*, 1324.
[5] F. E. Susan, K. L. Robert, *Chem. Phys. Lett.* **1994**, *218*, 349.
[6] G. T. Fraser, R. D. Suenram, F. J. Lovas, W. J. Stevens, *Chem. Phys.* **1988**, *125*, 31.
[7] B. M. Giuliano, L. B. Favero, A. Maris, W. Caminati, *Chem. Eur. J.* **2012**, *18*, 12759.
[8] S. J. Humphrey, D. W. Pratt, *J. Chem. Phys.* **1997**, *106*, 908.
[9] C. Tanner, C. Manca, S. Leutwyler, *Science* **2003**, *302*, 1736.
[10] B. M. Giuliano, S. Melandri, A. Maris, L. B. Favero, W. Caminati, *Angew. Chem.* **2009**, *121*, 1122; *Angew. Chem. Int. Ed.* **2009**, *48*, 1102.
[11] J. Sadlej, J. C. Dobrowolski, J. E. Rode, *Chem. Soc. Rev.* **2010**, *39*, 1478.
[12] G. Yang, Y. Xu, *J. Chem. Phys.* **2009**, *130*, 164506; M. Losada, P. Nguyen, Y. Xu, *J. Phys. Chem. A* **2008**, *112*, 5621.
[13] a) C. Merten, Y. Xu, *ChemPhysChem* **2013**, *14*, 213; b) C. Merten, Y. Xu, *Angew. Chem.* **2013**, *125*, 2127; *Angew. Chem. Int. Ed.* **2013**, *52*, 2073.
[14] H. Dreizler, H. D. Rudolph, H. Mäder, *Z. Naturforsch. A* **1970**, *25*, 25.
[15] I. Kleiner, J. T. Hougen, *J. Chem. Phys.* **2003**, *119*, 5505.
[16] S. Dempster, O. Sukhorukov, Q.-Y. Lei, W. Jäger, *J. Chem. Phys.* **2012**, *137*, 174303.
[17] PGOPHER, C. M. Western, University of Bristol, http://pgopher.chm.bris.ac.uk.
[18] Y. Xu, W. Jäger, *J. Chem. Phys.* **1997**, *106*, 7968.
[19] H. Hartwig, H. Dreizler, *Z. Naturforsch.* **1996**, *51*, 923.
[20] M. D. Marshall, J. S. Muenter, *J. Mol. Spectrosc.* **1981**, *85*, 322.
[21] A. C. Legon, *Chem. Soc. Rev.* **1993**, *22*, 153.
[22] A. van der Vaarta, K. M. Merz, Jr., *J. Chem. Phys.* **2002**, *116*, 7380.
[23] J. K. G. Watson in *Vibrational Spectra and Structure*, *Vol. 6* (Ed.: J. R. Durig), Elsevier, New York, **1977**, pp. 1–89.
[24] G. G. Brown, B. C. Dian, K. O. Douglass, S. M. Geyer, B. H. Pate, *J. Mol. Spectrosc.* **2006**, *238*, 200; G. S. Grubbs II, C. T. Dewberry, K. C. Etchison, K. E. Kerr, S. A. Cooke, *Rev. Sci. Instrum.* **2007**, *78*, 096106.
[25] T. J. Balle, W. H. Flygare, *Rev. Sci. Instrum.* **1981**, *52*, 33–45; J.-U. Grabow, W. Stahl, H. Dreizler, *Rev. Sci. Instrum.* **1996**, *67*, 4072.
[26] a) Gaussian 03 (Revision B.01), M. J. Frisch et al.; b) Gaussian 09 (Revision C.01): M. J. Frisch et al. See the Supporting Information for full references and comments on the calculations of the χ constants.
[27] S. F. Boys, F. Bernardi, *Mol. Phys.* **1970**, *19*, 553.